Journal of Sustainable Mining 15 (2016) 156–169

HOSTED BY

Contents lists available at ScienceDirect

Journal of Sustainable Mining

journal homepage: http://www.elsevier.com/locate/jsm

Assessment of process conditions associated with hydrodynamics of gas flow through materials with anisotropic internal structure

Grzegorz Wałowski [a, *], Gabriel Filipczak [b]

[a] Department of Renewable Energy Resources, Institute of Technology and Life Sciences, 67 Biskupińska Street, 60-463 Poznań, Poland
[b] Faculty of Mechanical Engineering, Chemical Engineering Department, Opole University of Technology, 5 Mikołajczyka Street, 45-271 Opole, Poland

ARTICLE INFO

Article history:
Received 11 January 2017
Accepted 18 March 2017
Available online 21 March 2017

Keywords:
Porous material
Char
Hydrodynamics
Gas flow
Anisotropy
UCG

ABSTRACT

The results of experimental research concerning the assessment of the permeability of porous materials with respect to gas flow are presented in this paper. The conducted research applied to, among others, chars (acquired from the UCG thermal process) with an anisotropic gap-porous structure and - for comparative purposes - model materials such as pumice and polyamide agglomerates. The research was conducted with the use of a special test stand that enables the measuring of gas permeability with respect to three flow orientations compared with symmetric cubic-shaped samples. The research results show the explicit impact of the flow direction on the permeability of chars, which results from their anisotropic internal structures. The suitability of calculation methods employed to calculate the hydrodynamics of the gas flow through porous materials was also evaluated.

1. Introduction

Gas flows through porous media in many process areas. These gas flows predominantly refer to gas filtration or gas flow through infilling layers as a porous medium with a loose arrangement. These flows are also encountered in technological processes concerning thermal carbon processing and during the flow of natural gases (e.g. methane) through rock masses and the flow of reactional gases through various chars such as coke, activated carbons, etc. (Błaszczyk, 2014; Stańczyk & Kapusta, 2011; Wiatowski et al., 2012; Woźnicka & Konieczyńska, 2013; Younger, 2011).

Contemporary technologies that use carbon as an energy raw material, increasingly refer to the possibility of using non-conventional processing technologies concerning the processing of carbon *in situ* (Smoliński, Stańczyk, Kapusta, & Howaniec, 2013). In these conditions the underground coal gasification process (UCG) occurs (Gregg & Edgar, 1978; Khadse, Qayyumi, Mahajani, & Aghalayam, 2007; Kreinin, & Zorya, 2009; Lapidusa et al., 2011), which produces gas that is suitable for energy purposes. This process leads to the creation of the so-called “char” that follows the partial or complete gasification of the carbon deposit (Kreinin, & Zorya, 2009; Stańczyk et al., 2012).

In certain technological processes the operation of apparatuses and the gas flow that occurs inside them is affected by the type and construction of gas phase distributors which are frequently made from porous materials (Zawora, 2001). In each case, the recognition of conditions of gas flow through porous deposits results in serious problems concerning the description of hydrodynamics and the evaluation of the mechanisms of gas flow through those deposits, particularly due to their diversified construction and internal structure. On the other hand, by being aware of those mechanisms, it is possible to evaluate the process conditions that accompany the hydrodynamics of gas flow through this type of materials, and, consequently, to thoroughly describe the hydrodynamic conditions of gas flow through materials and porous deposits. Although reference books widely analyse gas flow through porous materials, they do not clearly interpret and explicitly indicate the nature of the hydrodynamic phenomena accompanying this process. This mainly results from the highly complex and diversified structure of porous materials which – due to changeable flow conditions – leads to difficulties in interpreting these phenomena and also frequently due to the changeable process scale – from porous grains to porous deposits. In this field, reference books do not have models that describe the structural characteristics of porous materials resulting from their heterogeneous compositions. This situation becomes more complex with respect to the assessment of the hydrodynamics of the gas flow through solid materials with a porous (frame-structured) construction. At the same time, in this

* Corresponding author.
E-mail addresses: g.walowski@itp.edu.pl (G. Wałowski), g.filipczak@po.opole.pl (G. Filipczak).

http://dx.doi.org/10.1016/j.jsm.2017.03.003

field, it is difficult to find information on the hydrodynamics of gas flow through this type of porous materials. This study tackles some of these issues. The results of experimental research on the assessment of gas permeability of various solid porous materials have been presented and the assessment of process conditions concerning the hydrodynamics of gas flow through materials with an anisotropic internal structure has been conducted.

2. Materials and method

The research material comprises various types of solid frame-structure constructions, including those that are natural and those deriving from thermal carbon gasification technology. Of the latter, the largest group consists of chars *ex situ* and *in situ* (*in situ* chars result from underground hard coal gasification technology), melted waste rocks *ex situ*, coke, natural and synthetic pumice stones, and plastic porous agglomerates (gas distributor).

Chars *ex situ* that result from the partial or complete gasification of hard coal were obtained as part of the innovative project of the European Community of Coal and Steel with the acronym HUGE (*Hydrogen-oriented Underground Coal Gasification for Europe*) conducted by the Chief Mining Institute. The research on this issue was conducted in a surface reactor (*ex situ*) in which underground coal gasification conditions were simulated (Smoliński, Stańczyk, Kapusta, & Howaniec, 2012; Stańczyk et al., 2010). Hence, the research material obtained from that research was classified as biochar *ex situ*. The structure of these chars may be highly diversified, which affects the coal gasification degree (Janoszek, 2013; Stańczyk et al., 2011).

Chars *in situ* are direct products of underground coal gasification and they were acquired from the experimental georeactor (semi-technical scale) of the "Barbara" Experimental Mine (Stańczyk et al., 2012; Wiatowski et al., 2012). In this case, the process conditions enhanced the almost complete gasification of coal but the structure of this product is also extremely diversified, which – apart from process conditions – depends on the place where the sample is acquired from.

Melted waste rock (melted gangue rock) *ex situ* was acquired from deposits of the former Hard Coal Mine in Nowa Ruda near Wałbrzych (the Piast field). This rock is a semi-product of coal gasification in a shaft furnace designed for torrefying refractory shales (Kapuściński, 1968).

A separate group of experimental materials is coke. This material, as a char characteristic for the gasification of hard coal in a coke battery without air access, consists of hard coal products acquired from Poland and Australia and processed at the Zdzieszowice Coke Plant Arcelor Mittal Poland S.A. As numerous types of coke were used in our own research, to provide better readability, samples of this material were classified according to the names of the hard coal deposits.

Natural pumice (Vienna) consists of natural calcium carbonate with a small proportion of quartz sand and clay that derives from air-dried calcium slip (producer: *Top Choice*).

Whereas synthetic pumice is a product designed for cosmetic purposes and made from hard CFC-free polyurethane foam (manufacturer: 3M Poland Sp. z o.o.).

The last type of porous material employed in our own research is porous agglomerate (porous sinter). This material directly comes from the polymerization of spherical grained powders (manufacturer: Przedsiębiorstwo Wdrażania Innowacji "INWET" S.A.) and is used as a "gas distributor" designed for aerating liquid systems; other names for this are porous polyethylene or porous polyamide, depending on the type of plastics applied.

All the types of porous materials (samples) applied in this research underwent the assessment of selected parameters describing features that are characteristic for porous materials resulting from their porosity and physical structure as basic process quantities affecting the hydrodynamics of the gas flow through porous materials. The quantity-based assessment is applied to parameters such as the apparent density and porosity of a specific type (sample) of the porous material (Wałowski & Filipczak, 2012).

The parameters determined for the tested materials (samples) are outlined in Table 1 together with sample numbers and average values of those parameters.

The selected types of porous material also underwent physical assessment of their structure. This assessment was conducted on the basis of available SEM images (Wałowski, 2015).

The results lead to the conclusion that chars have highly diversified structures and their construction characteristics may be assigned to numerous porosity schemes. Chars *in situ* (Fig. 1a) generally have a gap structure with considerably large free spaces that are fundamental channels for gas flow. Whereas, the structure of coke (Fig. 1b) is characterised by a complex shape of numerous capillaries with variable cross-sections that are much more packed compared to the melted waste rock *ex situ* Fig. 1c. Finally, almost the entire volume of chars *ex situ* (Fig. 1d) is characterised by a gap-porous structure, hence they may be considered as a group of materials with a complex porosity system.

These observations confirm that the graphical identification of the structure of porous materials is a source of much more information that is suitable to assess the permeability of these materials when compared to their porosity degree.

2.1. Experimental stand

To obtain the research objective, detailed experimental tests were conducted to assess the gas permeability of porous materials with diversified structures (Fig. 1) and diversified process characteristics.

These tests applied to two independent gas permeability measurement systems as shown in Fig. 2, adjusted to the different shapes of the porous material samples.

The first system – Fig. 2a – is a measurement system designed for determining the permeability of materials in barbotage conditions. This measurement method is applied for samples with undefined shapes (volume ones) that resulted from naturally obtained parts of the samples. This enabled the assessment of the permeability intensity and the direction of the gas stream with respect to the sample surface.

The second measurement system – Fig. 2b – was applied to test the permeability of the same materials but these tests were conducted on cubic-shaped samples. In this system the gas flow was always directed with respect to the arbitrarily selected solid axis X, Y, Z.

In both cases, the working media applied in the gas permeability tests were air, nitrogen, and carbon dioxide. In each case, gas flowed through sample (1) in the free-pressure regime, the reference pressure in the pressure reducing valve (4) was (0.04-0.4) MPa and gas freely flowed out. Air was taken from the compressed air system, whereas nitrogen and carbon dioxide was supplied from gas bottles at the reference temperature of (17-25)°C. The decline in pressure in the specific measurement system was measured with differential pressure manometers (2) installed in the stream measurement system at the gas inlet to the material sample. The gas stream was measured with flota-controlled rotameters (3) scaled with the bellows gas meter before conducting the tests. For the remaining gases, relevant scale conversions were applied with respect to the correction co-efficient taking into consideration the change to state equation parameters. By using valves (5) to adjust

Table 1
Characteristic of research material.

Material (designation and source origin of raw material)		Porosity		Indicator porosity	Density	
Name	No. sample	Absolute	Effective		Apparent	Skeleton
		ε_b, %	ε_{ef}, %	e	ρ_{poz}, kg/m^3	ρ_{st}, kg/m^3
1	2	3	4	5	6	7
Char (carbonizer)*in situ*(KD Barbara, Mikolow)	I-1	42.2	21.1-33.7	0.7	1300	2250
	I-2	44.9	22.5-35.9	0.8	1239	
	I-3	33.9	17.0-27.1	0.5	1487	
	I – average	40.3	20.2-32.2	0.7	1342	2250
Coke(Zdzieszowice)	II-1	56.4	28.2-45.1	1.3	981	2250
	II-2	50.5	25.3-40.4	1.0	1113	
	II-3	49.8	24.9-39.8	1.0	1130	
	II – average	52.2	26.1-41.8	1.1	1075	2250
Coke(Illavarra)	II – 26 average	52.2	26.1-41.8	1.1	1075	2250
melted gangue *ex situ*(Nowa Ruda)	III-1	30.9	15.4-24.7	0.4	1365	1975
	III-2	19.3	9.6-15.4	0.2	1594	
	III-3	15.2	7.6-12.1	0.2	1675	
	III – average	21.8	10.9-17.4	0.3	1545	1975
Char (carbonizer) *ex situ*(KWK Piast)	IV-1	36.2	18.1-28.9	0.5	1436	2250
	IV-2	46.7	23.3-37.3	0.9	1200	
	IV-3	52.2	26.1-41.7	1.0	1076	
	IV – average	45.0	22.5-36.0	0.8	1237	2250
Natural pumice	XIII – average	63.3	31.7-50.7	1.7	843	2300
Synthetic pumice	XIV – average	88.1	44.1-70.5	7.4	106	900
sintered porous(polyamide)	XV – average	32.3	16.1-25.8	0.5	772	1140

the gas stream, permeability characteristics of the tested samples were determined for each system. All the results of the gas stream measurements were referred to as normal conditions (293 K, 1013 hPa).

Fig. 3 shows the applied sample supply system for the free gas flow (with the marking of the agreed parameters) and illustrates the gas conduct in these conditions.

In addition, Fig. 4 shows the method of supplying samples with an alternative shape that corresponds to the cubic solid of various sizes and whose front surface is sealed with a sealing material (from the side of the supply nozzle).

The shape of this type of sample together with a visible supply connection pipe (nozzle) is illustrated in Figs. 5 and 6. In the first figure, the images refer to the volume sample of char *in situ* (indefinite shape), whereas the second figure shows selected samples of cubic-shaped coke with a sealed front surface.

The measurement system, more strictly the construction of the permeability meter employed in the directed gas flow along the selected sample's axis X, Y, and Z, used for the cubic-shaped samples, is described in Fig. 7.

This specially designed permeability meter tests the permeability of cubic-shaped samples towards any direction of its axis, which is possible by applying a special sealing system to the measuring cell that enables the measuring of permeability in any direction (X, Y, Z) of the location of the measurement sample in the measurement system (Wałowski, Filipczak, & Krause, 2014) according to the scheme as shown in Fig. 2b.

The scheme of this measurement cell together with the marking of the sealing material and the measurement sample is shown in Fig. 8.

In each case, by using this type of permeability meter, permeability measurements were conducted independently with respect to the sample axis. In each measurement, the dimensions of the sample were 20 × 20 × 20 mm and this was cut out from a specific solid part of the test material. Therefore, the structural construction was specific for each type of porous material, which made it easier to compare hydrodynamic phenomena resulting from their gas permeability.

2.2. Scope and research methodology

To assess the hydrodynamics of gas flow through porous materials, tests were carried out with respect to volume samples with undefined shapes (Fig. 9a) and to cubic-shaped samples (Fig. 9b).

In both cases, the tests were conducted with reference to various gases (air, nitrogen, carbon dioxide) with regard to the permeability stream resulting from the reference pressure. Moreover, in both cases, the permeability function of the pressure decline in the porous deposit was independently determined, assuming the so-called multi-oriented (fractal) system for gas flow through samples with undefined shapes and the directional flow XYZ characteristic for cubic-shaped samples. Both cases are outlined in Fig. 10.

It is worth mentioning that for the cubic-shaped sample, permeability measurements were conducted independently for each selected flow direction by rotating this sample in the selected plane X, Y, Z of the measurement cell.

3. Results and discussion

The basis for assessing the hydrodynamics of gas flow through deposits and porous materials is the characteristic of their permeability resulting from the pressure that induces this flow. In each case, this characteristic is determined by calculating the impact of the available overpressure on the obtained gas stream or vice versa – the impact of the gas stream on the value of this overpressure that corresponds to a decline in this stream pressure. In the latter case, this corresponds to the determination of complete resistances of the gas flow through such deposit (Wałowski, & Filipczak, 2013).

The results shown in Fig. 11 and Fig. 12 prove that, with respect to porous materials in the form of char, the nature of the changes to gas permeability functions is highly diversified. For the same char *in situ* (Fig. 11) obtained highly different permeability characteristics have been obtained and their common deviation is expressly affected by the structure of the porous material. Moreover, those characteristics are parabolic, which proves their similarity to the hydrodynamics of the flow through the closed channels. On the

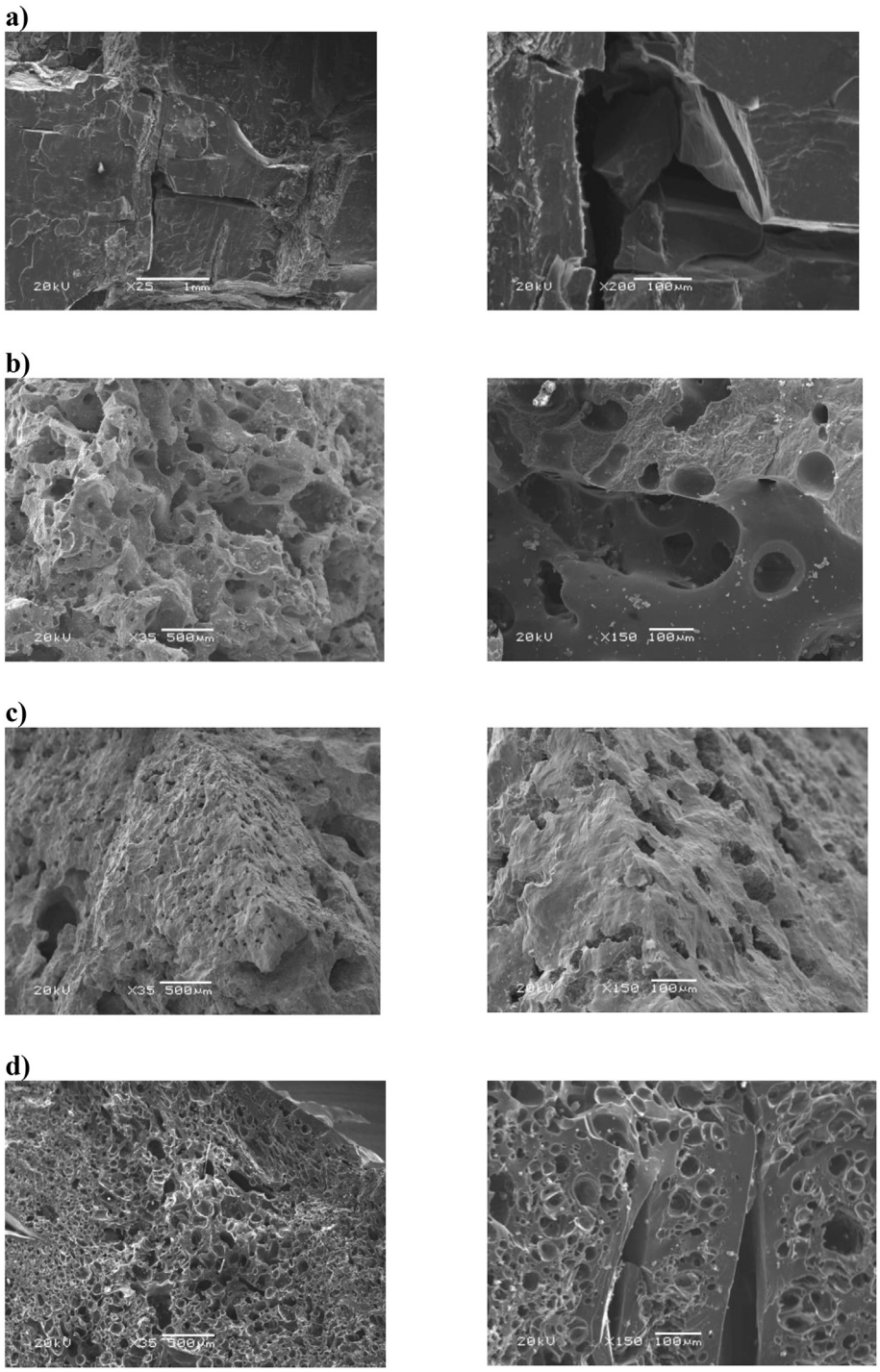

Fig. 1. SEM images of char structure in various magnifications: a) 1st sample – char *in situ*, b) 2nd sample – coke, c) 3rd sample – waste rock *ex situ*, d) 4th sample – char *ex situ.*

other hand, the non-linear tendency of those characteristics proves the dominance of the turbulent flow, which is also associated with deviation from Darcy's law.

The comparison to other materials, as shown in Fig. 12, shows that chars *in situ* (I-1, I-2, I-3) are porous structures which are much more permeable when compared to coke (II-1, II-2, II-3) or melted waste rock (III-1, III-2, III-3). As for coke with the highest porosity in this group the results prove that a large part of its pores is closed for gas flow and, concurrently, that chars with more complex structure have gap medium characteristics (Fig. 1a), which at the same reference pressure ensures much better gas permeability for this medium. On the other hand, in comparison with the aforementioned materials the permeability of the waste rock is undoubtedly justified by the relatively smaller porosity of this material and with their being less pores open for the flow (Fig. 1c).

Analogously, the permeability characteristics were made for samples of cubic-shaped porous materials with the use of the measurement system that enables the assessment of the permeability in the directed flow, i.e. according to the selected side plane of the solid (Fig. 10b). In geometrical form, thoee samples were

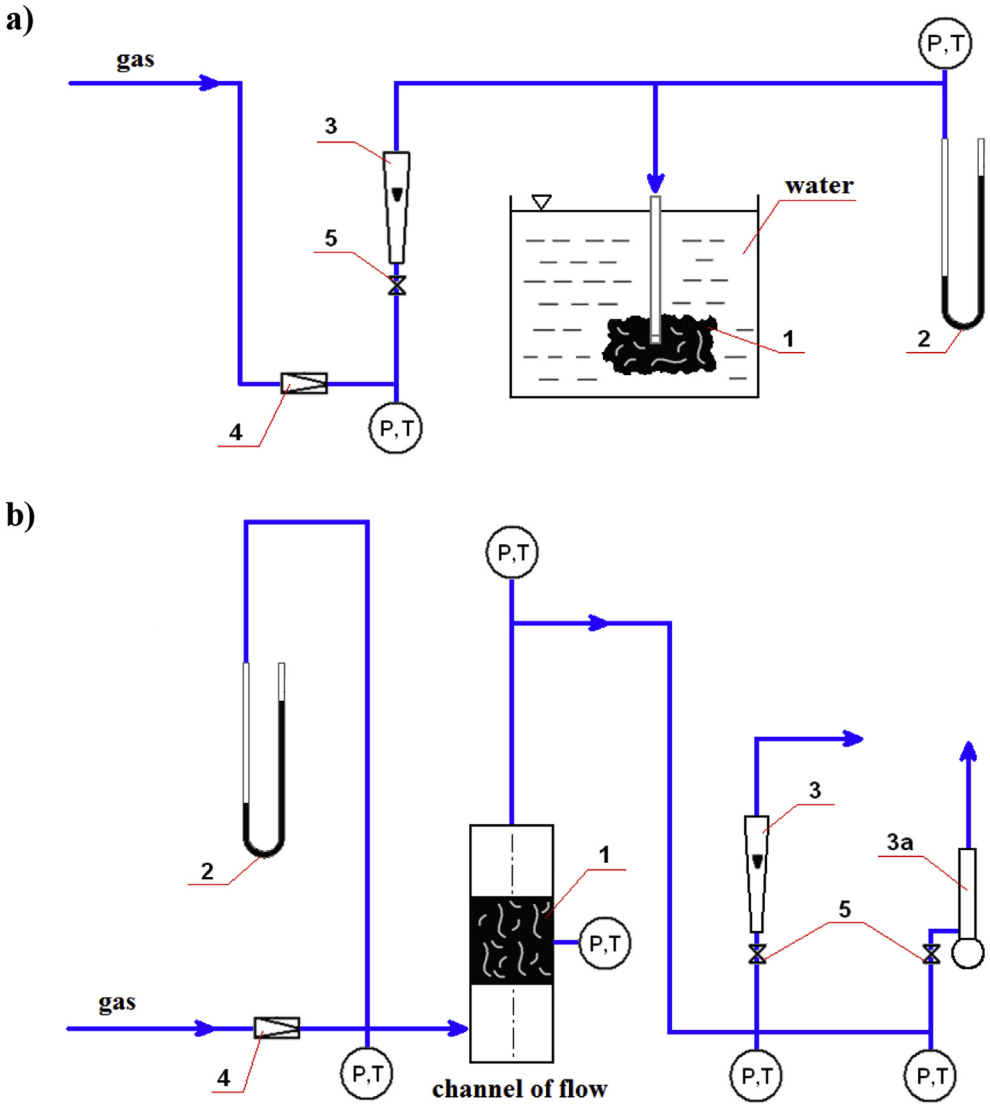

Fig. 2. Scheme of measurement system for porous material permeability tests: a) in barbotage conditions, b) for directed gas flow; 1 – porous material (sample), 2 – differential pressure manometer, 3 – rotameter (3a-bubble flowmeter), 4 – pressure redactors, 5 – control valve.

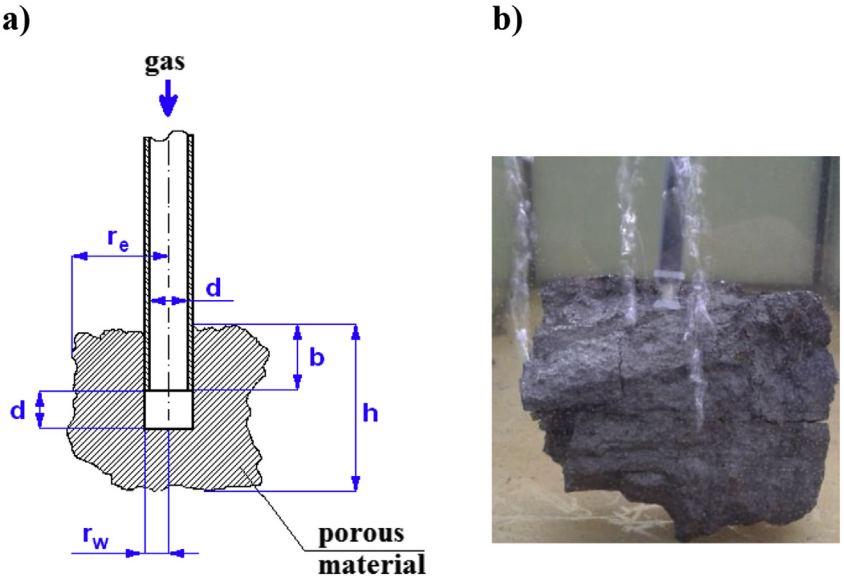

Fig. 3. Scheme of sample supply system (a) and gas flow in barbotage conditions (b).

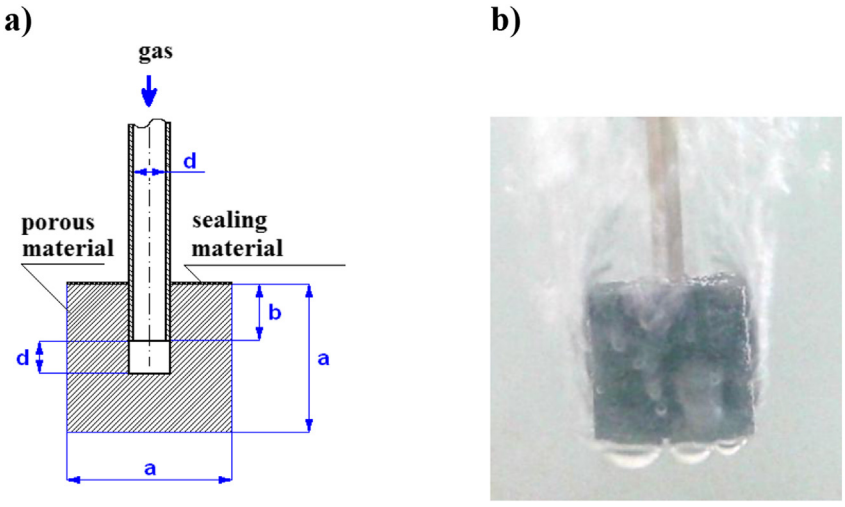

Fig. 4. Scheme of sample supply system with blind front plane (a) and its corresponding gas flow in barbotage conditions (b).

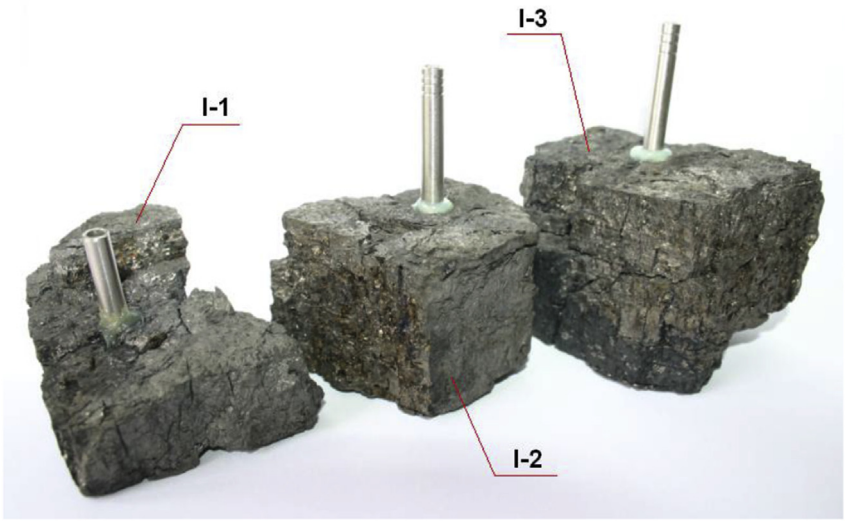

Fig. 5. Samples of porous material of different shapes – char *in situ* (I-1, I-2, I-3).

Fig. 6. Samples of cubic-shaped coke with a central nozzle: II-3A30 (30 × 30 × 30 mm), II-3A40 (40 × 40 × 40 mm), II-3A50 (50 × 50 × 50 mm).

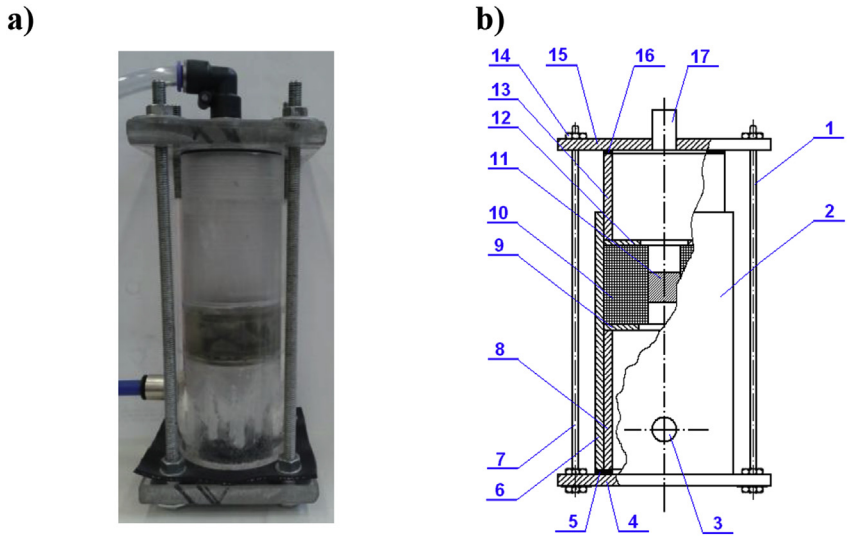

Fig. 7. Gas permeability meter: a) view, b) construction scheme: 1 – housing, 2 – cylindrical body, 3 – gas inlet pipe, 4 – bottom base, 5 – bottom gasket, 6 – motionless external bottom part, 7 – threaded rod, 8 – motionless internal bottom part, 9 – bottom back-up ring, 10 – measurement cell, 11 – porous material sample, 12 – upper back-up sample, 13 – movable upper bush, 14 – nut, 15 – upper base, 16 – upper gasket, 17 – gas outlet pipe.

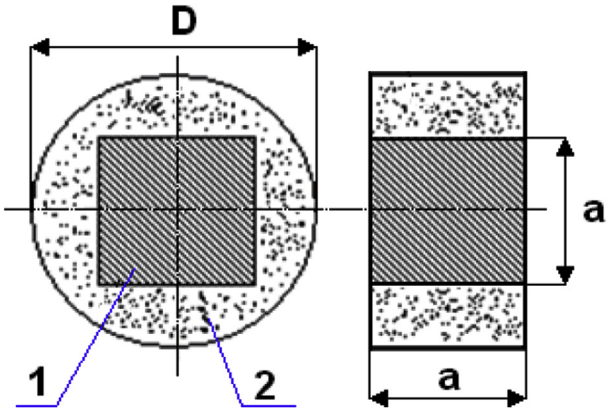

Fig. 8. Scheme of measurement cell: 1 – porous material, 2 – sealing material (cubic sample); D = 49 mm, a = 20 mm.

parts of volume samples and were compared with them with respect to their internal structure.

Selected results of the measurements of the cubic-shaped sample of char *in situ* are illustrated in Fig. 13a which shows characteristics of the air permeability of this material in three independent flow directions (X, Y, Z).

The distribution of experimental points shows that the permeability of this kind of material is considerably affected by the direction of the gas flow. This shows the explicit effect of the asymmetry of the permeability of the porous deposit with respect to the selected flow direction (axis) and, consequently, the explicit anisotropic structure of this type of material.

A reference point for the assessment of this asymmetry may be a porous polyamide comprising the agglomerate of spherical particles with identical dimensions (about 0.1 mm diameter). This material has absolute porosity of 32% (Wałowski & Filipczak, 2012) and its structure is similar to the rhombus-shaped system.

Fig. 9. Characteristic research material: a) volume sample with an undefined shape, b) cubic-shaped sample (defined shape).

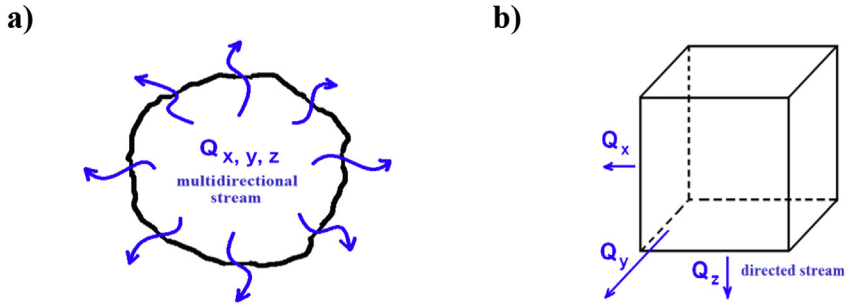

Fig. 10. Schemes of flow systems: a) multi-oriented – fractal (volume sample), b) oriented XYZ (cubic sample).

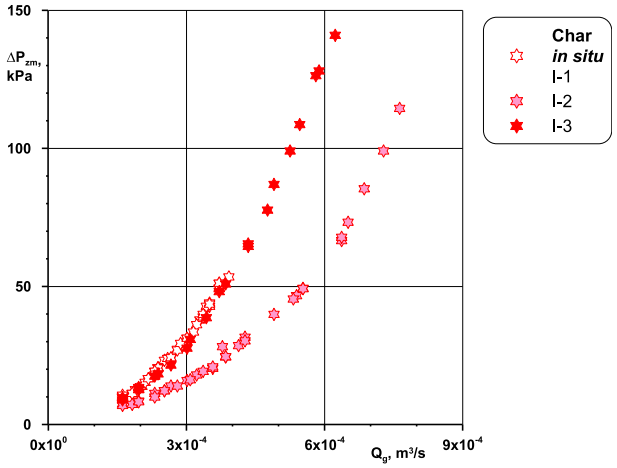

Fig. 11. Permeability of char *in situ* (volume sample).

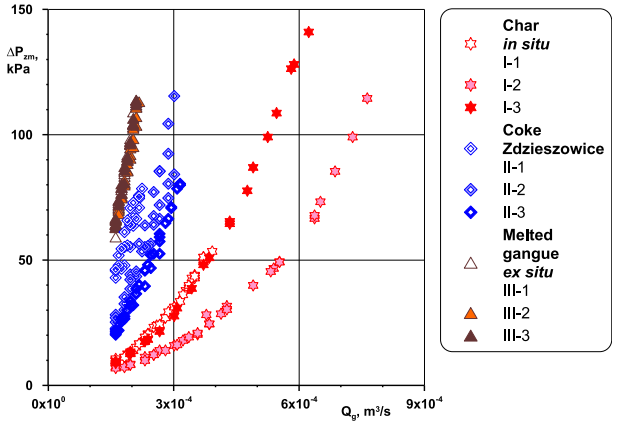

Fig. 12. Permeability of porous materials of various types (volume sample); (I – char *in situ*, II – coke (Zdzieszowice), III – melted waste rock *ex situ*).

The distribution of the experimental points shown in Fig. 13b proves that the permeability characteristics of this material do not practically depend on the direction of the gas flow, which proves the symmetrical structure of its construction. At the same time, characteristics determined for samples with the same dimensions (20 × 20 × 20 mm) prove that this polyamide, despite the fact that its porosity is much smaller compared to char (Wałowski, & Filipczak, 2013), has similar characteristics of gas flow. This supports the previous observation that the greater effect of the permeability of chars is mainly a result of their gap structure rather than their porosity. It is interesting that the permeability characteristic of the porous polyamide is also of non-linear nature, which - with respect to the measurements – proves the advantage of turbulent gas flow over laminar movement.

The essential conclusion arising from these observations is that the average permeability of the porous deposit is not affected by the shape of the fundamental deposit unit (sample) but by its internal structure, as proven by the research results. For example, Fig. 14 compares the characteristics of gas permeability determined for char *in situ* (I-1, I-2, I-3) in the same conditions of reference pressure between the volume sample and the cubic-shaped sample (the figure shows the average values of XYZ for the air flow). It can be noticed that the course of permeability characteristics of this material is similar in both cases and the geometrical shape of the sample does not have any specific impact on the obtained permeability of the porous deposit.

This is proven by the research results shown in Fig. 15 presenting permeability characteristics of air flow through coke with multiplied volume of cubic-shaped samples – 30 × 30 × 30, 40 × 40 × 40 and 50 × 50 × 50 mm (Fig. 6).

The results of those measurements show that the mutual deviation for gas permeability between the samples with many times greater volume does not lead to a proportional shift in permeability characteristics.

The experimental comparative characteristics of the permeability of various types of porous materials determined by using air, nitrogen and carbon dioxide are shown in Fig. 16 to Fig. 21. These characteristics referred to the cubic-shaped samples with uniform dimensions (20 × 20 × 20 mm).

Fig. 16 shows the experimental test results for char *in situ* that referred to the directional gas flow (X, Y, Z). Regardless of the detected anisotropy of this material, it may also be observed that for the entire extent of the reference pressure, the permeability of this char is less for air than for nitrogen but considerably higher than for carbon dioxide.

For this last gas (CO_2), the limitation of the permeability characteristics was also observed, which is certainly caused by the

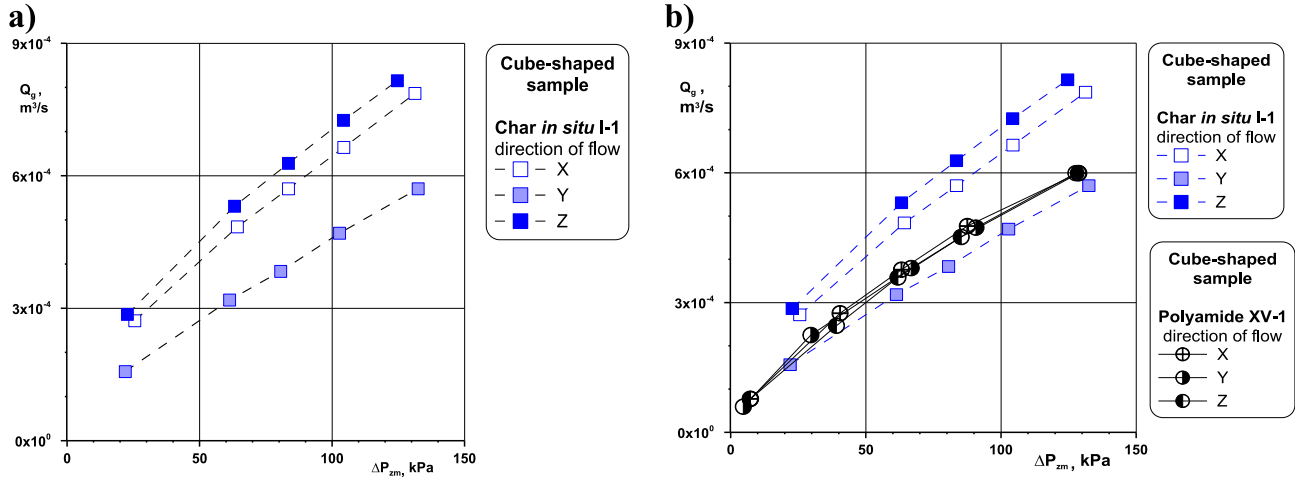

Fig. 13. Distribution of experimental points characterising asymmetry of air flow through a deposit of char *in situ* (a) and in comparison of this asymmetry to polyamide (b); cubic-shaped sample with dimensions of 20 × 20 × 20 mm.

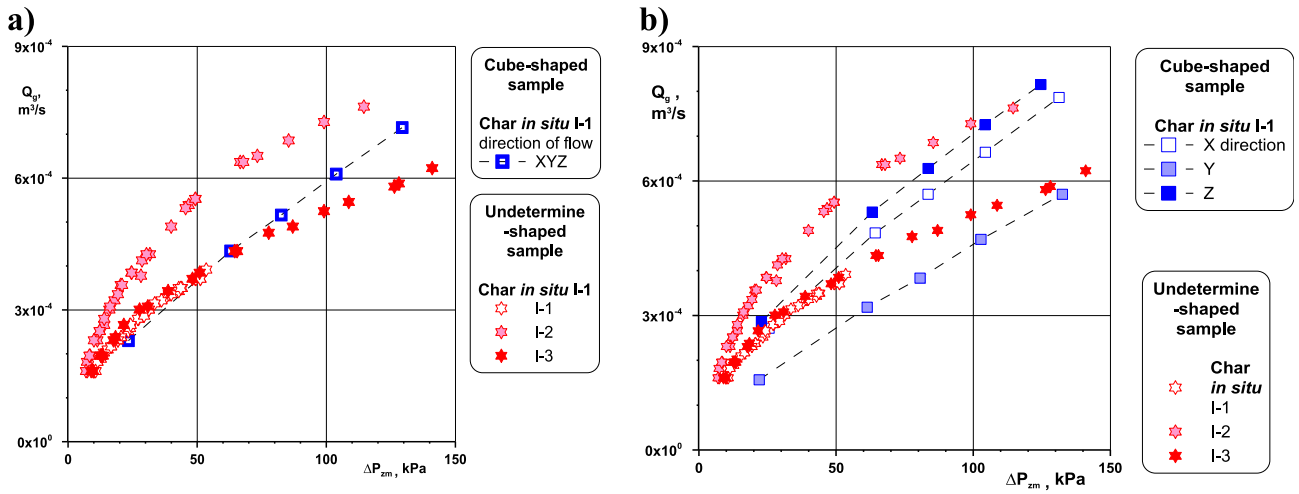

Fig. 14. Gas permeability of chars of various types and shapes: a) considering gas flow directions, b) average values for cubic-shaped sample.

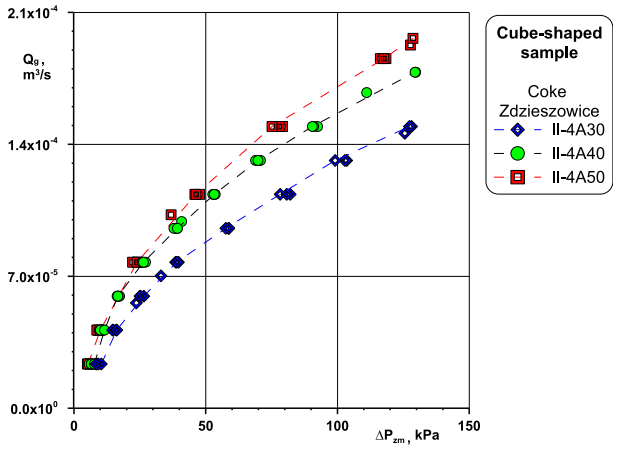

Fig. 15. Characteristics of permeability of coke with multiplied volume of cubic-shaped samples – air flow.

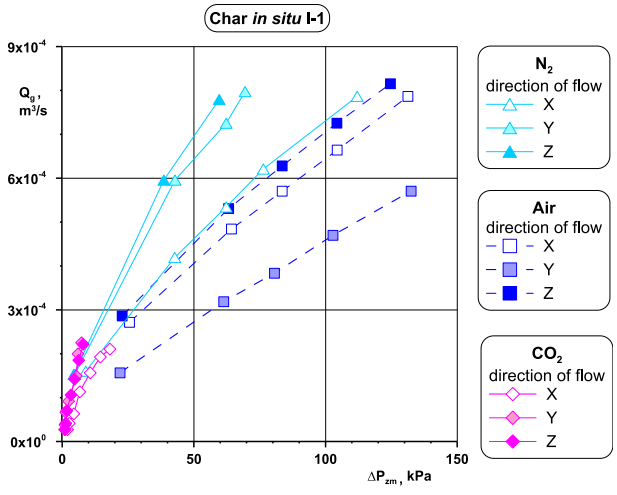

Fig. 16. Permeability of char *in situ* depending on working medium.

choking phenomenon that restricts the further increase in permeability, despite increasing the reference pressure. This may be affected by the fact that the density is higher compared with the remaining ones, but according to a fact proven in reference books (Michałowski & Wańkowicz, 1993; Ochęduszko, 1970) it is more likely that the hyphenation choking effect expressed by a pressure decline in the porous material is greater, the greater the resistance the gas flowing through the network of micro channels encounters (adiathermal conditions). On the other hand, other researchers (Blicharski & Smulski, 2012) suggest that the limitation of the permeability characteristics may be affected by the so-called Klingenberg effect – a phenomenon that limits the movement of gas molecules with sizes comparable to pore sizes. In this case, attention is drawn to the significance of this phenomenon in the aspect of the sequestration of carbon dioxide in geological deposits.

These observations prove the results of the measurements shown in Fig. 17 that refer to the average permeability of various kinds of materials that results from the directional streams (X, Y, Z) for the cubic solid.

It may be observed that, for air and nitrogen, polyamide (XV) and char *in situ* (I) have the highest permeability. Much lower permeability is observed for Illawarra coke (II-26) and for all gases

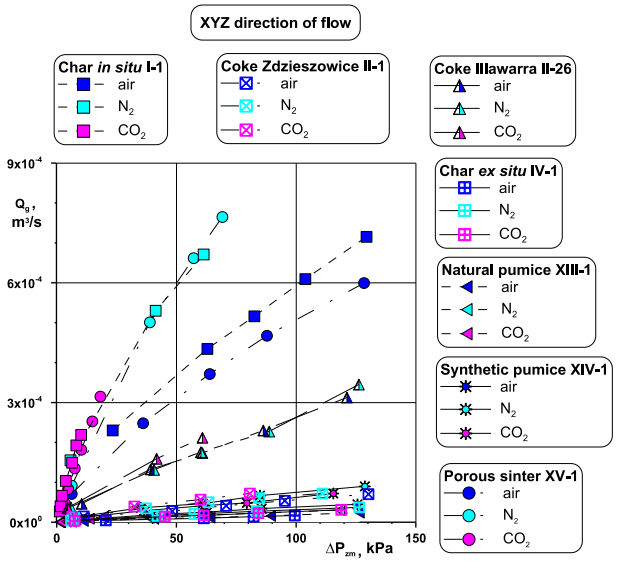

Fig. 17. Permeability characteristics of porous materials for air, nitrogen and carbon dioxide (cubic-shaped sample).

with similar flow characteristics, whereas this limit is much lower for the remaining materials. It is noteworthy that the limitation of carbon dioxide permeability is shown by all the materials which are affected by the reference pressure – e.g. for polyamide and char *in situ*, this pressure is about 20 kPa, whereas for Illawarra coke this pressure is about 60 kPa, and much higher for the remaining materials. The relatively high porosity of these materials (porosity of synthetic pumice is as high as 88%) means that free space is highly limited for gas flow, which is undoubtedly caused by a high share of pores that are blind and closed for flow in the structure.

A detailed list of the permeability measurement results for those materials with respect to gas flow direction (X, Y, Z) is shown in Fig. 18.

In general, in this case no essential deviation from the distribution of experimental points shown in the previous points is observed, but directional flow characteristics are more explicit and it is easier to notice common interdependences. Interestingly, towards the transversal direction of the flow Y (Fig. 18b), char *in situ*, polyamide and Illawarra coke have similar permeability characteristics with respect to air. In the remaining cases (directions X and Z) deviations between those characteristics are much greater, which is affected by the internal structure of the tested deposit and the type of the flowing gas.

The permeability characteristics determined separately for individual gases are shown in three drawings, respectively: Fig. 19 for air, Fig. 20 for nitrogen and Fig. 21 for carbon dioxide. In each case, the directional flow (X, Y, Z) refers to the same size of sample ($20 \times 20 \times 20$ mm) and to the same arrangement of the sample with respect to the gas flow direction.

By comparing experimental points it is possible to determine that characteristics closest to the isotropic structure are only shown in polyamide, however its permeability characteristics for individual gases are different and its highest permeability (for the same reference pressure) is obtained for the flow of nitrogen. It may be assumed that these characteristics are shown by materials like pumice but their very low permeability does not provide a clear

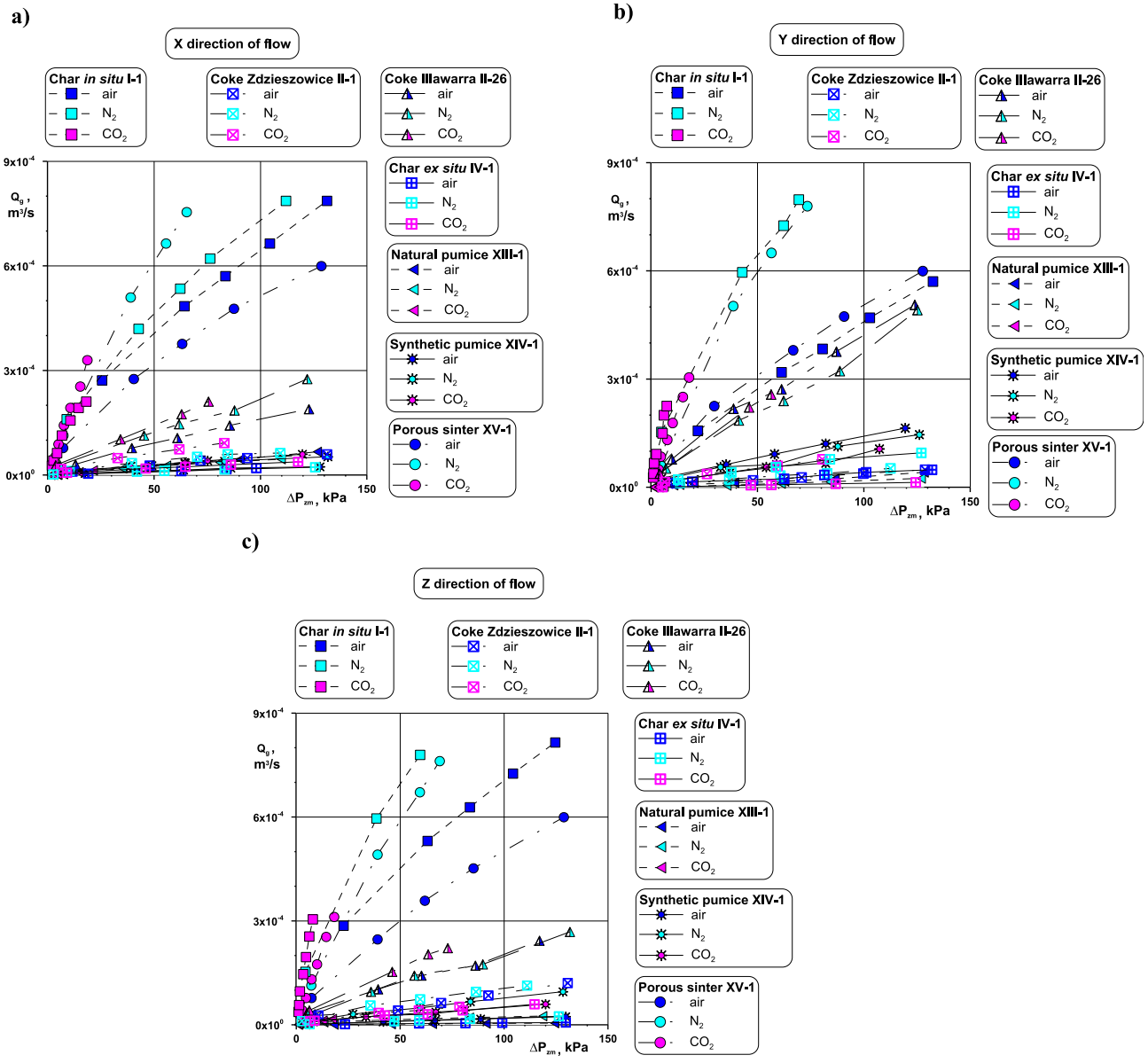

Fig. 18. Permeability of porous materials for air, nitrogen and carbon dioxide depending on direction of gas flow (cubic-shaped sample): a) flow direction X, b) flow direction Y, c) flow direction Z.

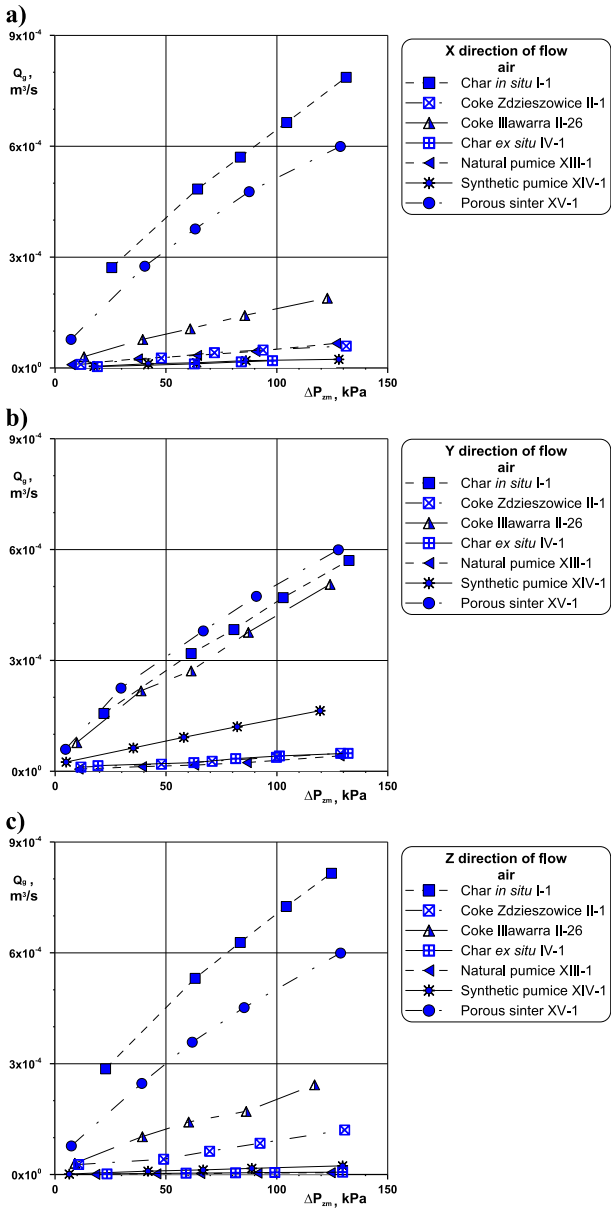

Fig. 19. Permeability characteristics of porous materials for air (cubic-shaped sample): a) flow direction X, b) flow direction Y, c) flow direction Z.

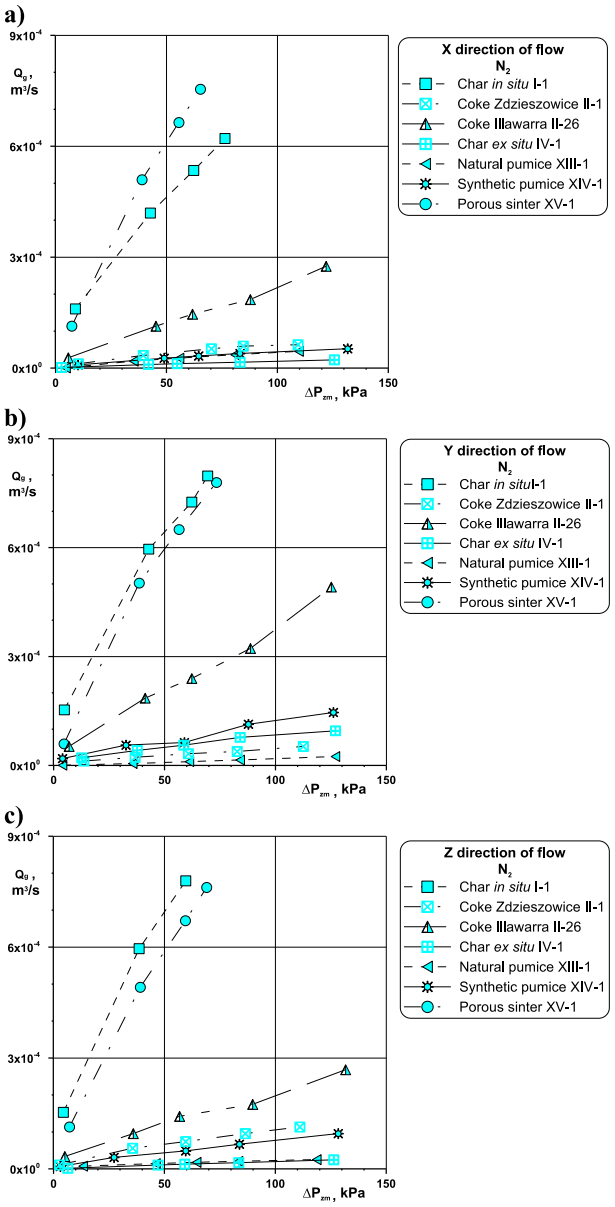

Fig. 20. Permeability characteristics of porous materials for nitrogen (cubic-shaped sample): a) flow direction, b) flow direction Y, c) flow direction Z.

assessment in this case. In all the other cases, with reference to individual flow directions, the permeability characteristics refer to the explicit anisotropy of the structure of the tested materials, in particular chars and cokes.

In addition, it can be seen that the flow characteristics determined for directions X and Y present a similar tendency which is much more convergent than for direction Z. This undoubtedly results from the fact that the flow directed for the cubic solid occurs in two mutually perpendicular planes - horizontal for directions X and Y and vertical for direction Z (Fig. 10). In this first case (X, Y) the structural cross-sections are much more similar to each other than when either is compared with the perpendicular cross-section.

It is noteworthy that the characteristics of gas permeability through the porous material are directly associated with the values of the pressure decline that occurs in a particular porous deposit for a specific gas stream.

By using these considerations, Table 2 contains selected models (correlation equations) which were applied to assess their suitability for the calculation of flow resistances by the tested porous materials.

To verify the suitability of these models for the description of the results obtained in our own research, model equations and their parameters were properly adapted to the conditions resulting from the specificity of our own research. The obtained results are shown in Fig. 22 that compares the values calculated from the models with the measured values.

According to the distribution of the experimental points for all the analysed conditions, for both the directional flow (X, Y, Z) and the averaged flow, the equations included in Table 2 are not in line with the description of the hydrodynamics of the tested porous materials. The distribution of the experimental points considerably differs from the calculated values, towards higher and lower values. It can be observed, however, these values are defined in sufficient

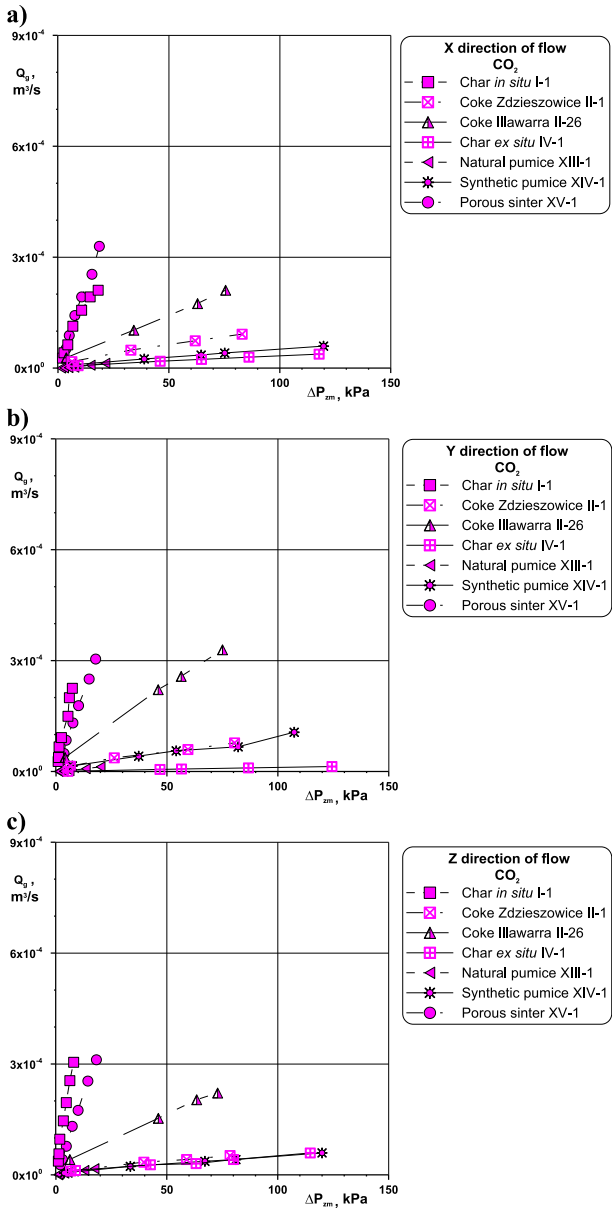

Fig. 21. Permeability characteristics of porous materials for carbon dioxide (cubic-shaped sample): a) flow direction X, b) flow direction Y, c) flow direction Z.

detail by Windsperger's model (5) only for direction X (Fig. 22a) and by Ergun's model (3) for direction Y (Fig. 22b). However, for the averaged results (Fig. 22d) both of these models provide values that are considerably different than the measured ones, which also refer to the remaining methods.

The results of this comparison show that the possible adaptation of calculation methods (models), which are characteristic for porous grained deposits, does not have sufficient circumstances to employ these methods in the description of the hydrodynamics of the gas flow through frame-structured (solid) porous deposits. The main reason for this state of affairs can be ascribed to the fact that frame-structured porous materials are characterised – as proven by our own research – by gas permeability that is disproportionately lower than the calculated value as shown in a potential porosity scale of this material. As emphasised many times, this is caused by numerous pores that are blind and closed for gas flow occurring in porous frame-structured materials. In effect, pressure losses in the deposit of the frame-structured material, both those that may be associated with friction losses and losses caused by the speed profile disturbance (local), differ from those that are characteristic for flow with a complete cross-section resulting from the deposit's porosity.

4. Conclusions

The results of this research on permeability lead to a number of conclusions. Chars have a highly diversified structure and their construction characteristics may be assigned to numerous porosity schemes.

The graphical identification of the structure of porous materials is a source of much more information which is useful when assessing the permeability of these materials rather than the porosity degree.

Chars *in situ* (gap medium) are porous structures that are much more permeable than coke (highest porosity) or melted waste rock (lower porosity – small share of open pores).

The average permeability of the porous deposit does not depend on the shape of the fundamental deposit unit (sample) but depends on its internal structure.

The comparative characteristics of the permeability of various porous materials, determined by using air, nitrogen and carbon dioxide, prove that the flow choking phenomena, caused by the much greater density of carbon dioxide compared with the remaining gases, occurs. The isenthalpic choking effect which becomes larger, the larger resistance the gas encounters while flowing through the network of micro-channels (in adiathermal conditions), also occurs. Whereas, the so-called Klingenberg effect occurs as a phenomenon that limits the movement of gas molecules whose sizes are comparable with pore sizes (the aspect of sequestration of carbon dioxide in geological deposits).

The flow directed for the cubic solid occurs in two mutually perpendicular planes – horizontal for directions X and Y and vertical for direction Z.

Table 2
Method of calculating resistances (pressure drop) of flow through porous materials.

Author	Correlation equation	
Brauer (Brauer, 1971)	$\Delta P_B = \xi_B \cdot \Delta P_E \cdot \left(\frac{(1-\varepsilon)^2}{\varepsilon^3} \cdot \frac{v_r \cdot \eta}{d_z} \cdot H \right)$	(1)
Carman (Carman,1956)	$\Delta P_C = \frac{\eta \cdot v_r \cdot H}{B_o};\ B_o = \frac{d_z^2}{16 \cdot k} \cdot \frac{\varepsilon^3}{(1-\varepsilon)^2};\ k = 2 \cdot \varphi_\varepsilon$	(2)
Ergun (Ergun,1952)	$\Delta P_E = \left(150 \cdot \frac{(1-\varepsilon)^2}{\varepsilon^3} \cdot \frac{v_r \cdot \varepsilon}{d_z^2} \cdot H \right) + \left(1,75 \cdot \frac{(1-\varepsilon)^2}{\varepsilon^3} \frac{v_r^2 \cdot \rho}{d_z} \cdot H \right)$	(3)
Leva (Mokrosz,1996)	$\Delta P_L = \alpha \cdot \rho \cdot v_\varepsilon^2 \cdot H;\ \alpha = \frac{1,75}{4 \cdot \sqrt{k} \cdot \varepsilon^{1,5} \cdot \sqrt{B_o}}$	(4)
Windsperger (Windsperger, 1991)	$\Delta P_W = \frac{3}{4} \cdot \xi W \cdot \left(\frac{(1-\varepsilon)}{\varepsilon^3} \cdot \frac{\rho \cdot v_r^2}{d_z} \cdot H \right)$	(5)
Zaworonkow (Zaworonkow, 1944)	$\Delta P_Z = \frac{2 \cdot \xi_Z \cdot \rho \cdot v^2 \cdot H}{\varepsilon^2 \cdot d_z}$	(6)

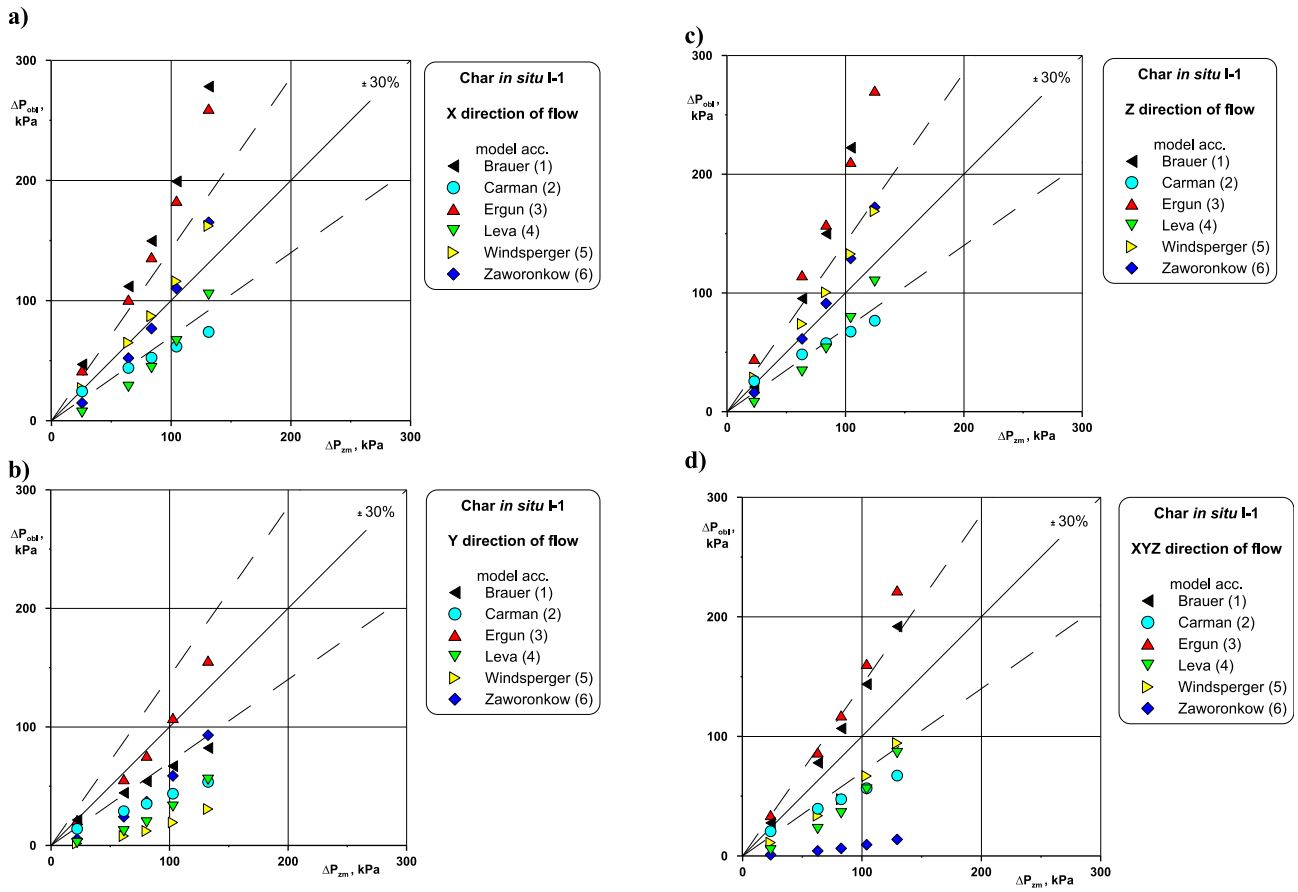

Fig. 22. Comparison of values of measured gas flow resistances with calculated values – char *in situ* (cubic-shaped sample): a) direction X, b) direction Y, c) direction Z, d) average value XYZ.

The characteristics of gas permeability through the porous material are directly associated with the values of the pressure decline that occurs in a particular porous deposit for a specific gas stream.

The relevant adaptation of model equations and their parameters to the conditions arising from the specificity of our own research proves that the distribution of the experimental points considerably differs from the calculated values, towards higher and lower values.

There are not sufficient circumstances to employ the possible adaptation of calculation methods (models) characteristic for porous grained deposits in the description of hydrodynamics of gas flow through frame-structured (solid) porous deposits, i.e. chars.

Acknowledgements

The study was conducted as part of a project financed by the National Centre for Research and Development conducted in the BIOSTRATEG program, contract No BIOSTRATEG2/298357/8/NCBR/2016 dated 18 May 2016.

References

Blicharski, J., & Smulski, R. (2012). Stanowisko laboratoryjne wypierania się płynów w ośrodkach porowatych w aspekcie sekwestracji CO2 [Laboratory apparatus for fluids displacement in porous media in aspect of carbon dioxide sequestration]. *AGH Drilling, Oil, Gas, 29*(1), 89–96.

Brauer, H. (1971). *Grundlagen der Einphasen – und Mehrphasenströmungen*. Frankfurt am Main: Verlag Säuerländer.

Błaszczyk, M. (2014). *Badanie procesów migracji substancji ropopochodnych i ich emulsji w strukturach porowatych: Praca dokotorska [Research upon processes of migration of petroleum substances and their emulsions in porous structures. Doctoral thesis]. Łódź: Politechnika Łódzka, Wydział Chemiczny*.

Carman, P. C. (1956). *Flow of gases through porous media*. London: Butterworths Sc. Public.

Ergun, S. (1952). Fluid flow through packed columns. *Chemical Engineering Progress, 48*(2), 89–94.

Gregg, D. W., & Edgar, T. F. (1978). Underground coal gasification. *American Institute of Chemical Engineers Journal, 24*, 753–781.

Janoszek, T. (2013). Exergy analysis of the coal gasification process in ex-situ conditions. *Journal of Sustainable Mining, 12*(3), 32–37.

Kapuściński, T. (1968). *Charakterystyka mineralogiczno-chemiczna i geneza łupków ogniotrwałych z Kopalni Nowa Ruda [Mineralogical-chemical characteristics and genesis of refractory shales from the Nowa Ruda Mine]. Prace Geologiczne 51*. Warszawa: Wydawnictwo Geologiczne.

Khadse, A., Qayyumi, M., Mahajani, S., & Aghalayam, P. (2007). Underground coal gasification: A new clean coal utilization technique for India. *Energy, 32*(11), 2061–2071.

Kreinin, E. V., & Zorya, A. Yu (2009). Underground coal gasification problems. *Solid Fuel Chemistry, 43*, 215–218.

Lapidusa, A. L., Katorginb, B. I., Eliseeva, O. L., Kryuchkova, M. V., Kreininc, E. V., & Volkova, A. S. (2011). Hydrocarbon synthesis from a model gas of underground coal gasification. *Solid Fuel Chemistry, 45*(3), 165–168.

Michałowski, S., & Wańkowicz, K. (1993). *Termodynamika procesowa [Process thermodynamics]*. Warszawa: WNT.

Mokrosz, W. (1996). *Badania procesu absorpcji SO2 w absorberach alkalicznych z wykorzystaniem współprądowego aparatu z wypełnieniem komórkowym. Praca doktorska [Research on the SO2 absorption process in alkaline absorbers by using a parallel flow apparatus with cellular packing. Doctoral thesis]*. Gliwice: Politechnika Śląska.

Ochęduszko, S. (1970). *Applied thermodynamics*. Warszawa: WNT.

Smoliński, A., Stańczyk, K., Kapusta, K., & Howaniec, N. (2012). Chemometric study of the ex situ underground coal gasification wastewater experimental data. *Water, Air & Soil Pollution, 223*, 5745–5758.

Smoliński, A., Stańczyk, K., Kapusta, K., & Howaniec, N. (2013). Analysis of the

organic contaminants in the condensate produced in the in situ underground coal gasification process. *Water Science & Technology, 67*(3), 644–650.
Stańczyk, K., Howaniec, N., Smoliński, A., Świądrowski, J., Kapusta, K., Wiatowski, M., et al. (2011). Gasification of lignite and hard coal with air and oxygen enriched air in a pilot scale ex situ reactor for underground gasification. *Fuel, 90*, 1953–1962.
Stańczyk, K., & Kapusta, K. (2011). Pollution of water during underground coal gasification of hard coal and lignite. *Fuel, 90*(5), 1927–1934.
Stańczyk, K., Kapusta, K., Wiatowski, M., Świądrowski, J., Smoliński, A., Rogut, J., et al. (2012). Experimental simulation of hard coal underground gasification for hydrogen production. *Fuel, 91*, 40–50.
Stańczyk, K., Smoliński, A., Kapusta, K., Wiatowski, M., Świądrowski, J., Kotyrba, A., et al. (2010). Dynamic experimental simulation of hydrogen oriented underground coal gasification. *Fuel, 89*, 3307–3314.
Walowski, G., & Filipczak, G. (2013). Ocena hydrodynamiki przepływu gazu przez ośrodek szczelinowo-porowaty (Assessment of hydrodynamics of gas flow through gap-porous material). *Inżynieria i Aparatura Chemiczna, 52*(6), 581–582.
Wałowski, G. (2015). *Hydrodynamika przepływu gazu przez złoże porowate. Praca doktorska [hydrodynamics of gas flow through porous deposits. Doctoral thesis]*. Opole: Politechnika Opolska.
Wałowski, G., & Filipczak, G. (2012). Ocena przepuszczalności materiału porowatego w warunkach barbotażu [Assessment of permeability of porous materials in barbotage conditions]. *Inżynieria i Aparatura Chemiczna, 51*(6), 396–397.
Wałowski, G., Filipczak, G., & Krause, E. (2014). *Układ do wyznaczania współczynnika przepuszczalności gazów przez porowate materiały o anizotropowej strukturze, zwłaszcza przez karbonizaty [System for determination the coefficient of gas permeability through porous materials with anisotropic structure, preferably through chars]. Patent application P.409191*. Warsaw: Patent Office of the Republic of Poland.
Wiatowski, M., Stańczyk, K., Świądrowski, J., Kapusta, K., Cybulski, K., Krause, E., et al. (2012). Semi-technical underground coal gasification (UCG) using the shaft method in Experimental Mine "Barbara". *Fuel, 99*, 170–179.
Windsperger, A. (1991). Abschätzung von spezifischer Oberfläche und Lückengrad bei biologischen Abluftreinigungsanlagen durch Vergleich von berechneten und experimentell erhaltenen Druckverlustwerten. *Chemie Ingenieur Technik, 63*(1), 80–81.
Woźnicka, M., & Konieczyńska, M. (2013). Eksploatacja gazu z łupków a środowisko naturalne [Exploitation of shale gas and natural environment]. In E. Sarnecka (Ed.), *Państwowa służba geologiczna o gazie w łupkach [State geological authority about shale gas]* (pp. 94–101). Warszawa: Państwowy Instytut Geologiczny – Państwowy Instytut Badawczy.
Younger, P. L. (2011). Hydrogeological and geomechanical aspects of underground coal gasification and its direct coupling to carbon capture and storage. *Mine Water and the Environment, 30*(2), 127–140.
Zawora, J. (2001). *Basics for machine engineering*. Warszawa: WSiP.
Zaworonkow, M. N. (1944). *Gidrawliczeskije osnowy skrubbernogo processa i tiepłopieredacza w skrubberach*. Moscow: Izd. Nauka.